Plasmonics (2017) 12:1221–1225
DOI 10.1007/s11468-016-0379-y

Synthesis and Optical Properties of Highly Stabilized Peptide-Coated Gold Nanoparticles

P. Kalakonda [1,2] · **B. Sreenivas** [3]

Received: 10 May 2016 / Accepted: 11 September 2016 / Published online: 28 September 2016

Abstract The interaction between peptide and gold nanoparticle surfaces has been increasingly of interest for bionanotechnology applications. To fully understand how to control such interactions, we have studied the optical properties of peptide-modified gold nanoparticles. However, the impacts of peptide binding motif upon the surface characteristics and physicochemical properties of nanoparticles remain poorly understood. Here, we have prepared sodium citrate-stabilized gold nanoparticles and coated with peptide IVD (ID_3). These nanomaterials were characterized by UV-visible, transmission electron microscopy (TEM), and z-potential measurement. The results indicate that gold-peptide interface is generated using ID_3 peptide and suggested that the reactivity of peptide is governed by the conformation of the bound peptide on the nanoparticle surface. The peptide-nanoparticle interactions could potentially be used to make specific functionality into the peptide capped nanomaterials.

Keywords Gold nano particles · Peptides · Z-potential · Optical properties

Electronic supplementary material The online version of this article (doi:10.1007/s11468-016-0379-y) contains supplementary material, which is available to authorized users.

✉ P. Kalakonda
parvathalu.k@gmail.com; pkalakon@cmu.edu

[1] Department of Materials Science and Engineering, Carnegie Mellon University, Pittsburgh, PA 15213, USA

[2] Department of Physics, Indian Institute of Science, Bangalore, KA, India

[3] Department of Chemistry, Chongqing University, Chongqing 401331, China

Introduction

Recently, the synthesis of stable gold nanoparticles is one of the most leading active researches in the field of nanotechnology because of their applications in broader areas such as bioimaging, biomedicine, biolabels, biosensors, catalysis, biomedical, drug delivery, and diagnostics [1–8]. The metal nanoparticle systems must be capped appropriately to render them biocompatible, functional, and stable against aggregation in biological systems [9, 10]. A current main challenge is maintaining size and size distribution upon introduction into biological environment. Ideally, the nanoparticle size should be larger than 10 nm to avoid renal clearance [11] and below 100 nm with a neutral or negative charge to avoid phagocytic uptake. The protein adsorption can drastically alter the physicochemical properties of nanoparticles and affect their circulation, biodistribution, and cellular internalization [12]. In addition, opsonization can result in undesired cellular uptake, nanoparticle aggregation, or an immune system response [13].

Current methods for creating "stealth" nanoparticles that resist nonspecific protein adsorption include surface modification by polyethylene glycol (PEG) [14], polysaccharides [15], mixed charge self-assembly [16], and polymers [17, 18]. An attractive way for stealth coatings is to study the use of natural materials such as peptides: they are biocompatible, biodegradable, well-studied, nonimmunogenic, and multifunctional materials [19]. Peptide-coated gold nanoparticles (PC-GNP) have been studied to make stable systems in phosphate-buffered saline (PBS) [20, 21]. However, achieving stability in complex media such as undiluted human serum is even more challenging than in PBS due to the presence of thousands of proteins. PC-GNPs have also been studied for in vivo applications [22, 23]. The effect of interactions between PC-GNPs and peptides were not fully studied. It is required or essential to study particles in complex media

solutions before performing in vivo experiments. Developing PC-GNPs that are stable in complex media can broaden in vivo applications and provide additional low fouling materials. In addition to possessing stealth properties, it is useful to incorporate specific interactions for biomedical technology applications. Many peptide sequences possess specific molecular recognition for receptors on various cell types. However, additional conjugation steps are needed to add peptide targeting sequences onto stealth particles containing synthetic low fouling polymers such as PEG [24, 25]. Peptide coatings offer an advantage because the targeting sequence can simply be extended off the existing peptide sequence [26, 27] avoiding complex conjugation steps. Combining the stealth peptide sequence with a targeting moiety achieves specific interactions while maintaining a low fouling background leading to increased stability in complex media and improved functionality.

In this work, we have designed a synthetic peptide of IVD (ID3) [28] associated with amyloid disease. This indicates a strong hydration layer providing resistance to nonspecific protein adsorption [29]. Furthermore, the sequence mimics the surfaces of proteins which have adapted to avoid nonspecific adsorption and display stability in complex media. Overall charge neutrality is maintained by leaving the N-terminus as a free amine, which contributes an extra positive charge to the peptide. The peptide sequence was attached to gold nanoparticles (GNP) through the inclusion of a surface anchoring via covalent bonding to the gold surface. Optical spectroscopy (UV-visible) and zeta potential results indicate peptide capped gold nanoparticles display high stability. This multifunctional peptide contains biomolecular recognition, ultralow fouling, and surface anchoring in one sequence. Moreover, this system is easily constructed in a one-step process by mixing gold nanoparticles and self-assembling peptides.

Experimental Section

Materials and Methods

Gold (III) chloride ($HAuCl_4$) and citric acid tri-sodium salt dehydrate were bought from Fisher Scientific (Waltham, MA). Peptide (ID3) with confirmed amino acid analysis (purity ≥95 %) was purchased from the American Peptide Company. Net peptide content varied between 70 and 85 %. The ID3 peptide was acetylated at the N-terminus. All solvents were purchased from Sigma-Aldrich Co. All these chemicals were analytical grade and used without any further purification.

Citrated Capped Gold Nanoparticle Synthesis Gold nanoparticles were synthesized by reduction of $HAuCl_4$ with citric acid. The aqueous solution of 0.5 mM HAuCl4 was vigorously stirred and heated until it steaming. To prepare 13-nm-diameter AuNPs, 25 mL solution of 38.8 mM solution was heated to reflux under stir and then sodium citrate solution was added quickly (25 mL, 38.8 mM). After color changing to red, the solution heated for another 10–15 min. The final reddish solution was allowed to cool naturally to room temperature (Fig. 1).

Peptide-Coated GNPs Peptide-coated GNPs were prepared by mixing citrated capped GNP with 0.5 mM peptide in aqueous solution. The solution was stirred for 10 min, and the self-assembled process was performed for 24 h.

Characterization of Gold Nanoparticles UV-visible absorption spectra were recorded at room temperature with a Smart Spec 3000 spectrophotometer from 300 to 800 nm. Fluorescence emission spectra were collected using a Horiba Fluoromax-4 spectrofluorometer. The chemical compositions of GNPs solution were collected by using a Fourier transform infrared spectroscopy (FTIR-6700 Smart FTIR spectrometer ranging from 4000 to 400 cm^{-1}). The gold nanoparticles size and morphology of particles was determined by TEM using a Tecnai G2 F20. Samples were prepared by evaporating 10 μL of GNP solution onto carbon-supported copper grids. For the determination of particle size, over 300 particles were counted from multiple pictures from different areas of the TEM grid using ImageJ software. The zeta potential of the particles was analyzed by using the Zetasizer Nano-ZS. Measurements were carried out at 25 °C in aqueous media. The zeta potential was calculated from the electrophoretic mobility based on the Smoluchowski theory.

Results and Discussion

The citrated-GNPs and peptide-coated GNPs were characterized by transmission electron microscopy (TEM) (Fig. 2). The

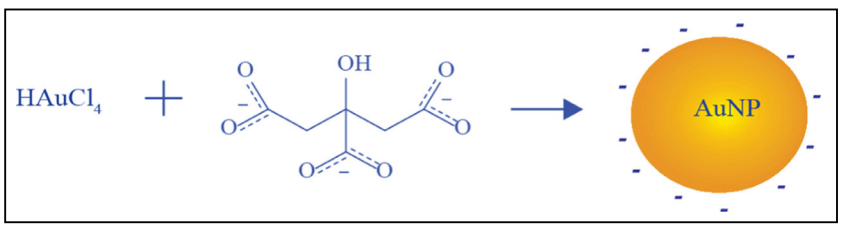

Fig. 1 Schematic of silver nanoparticles (GNPs) synthesis

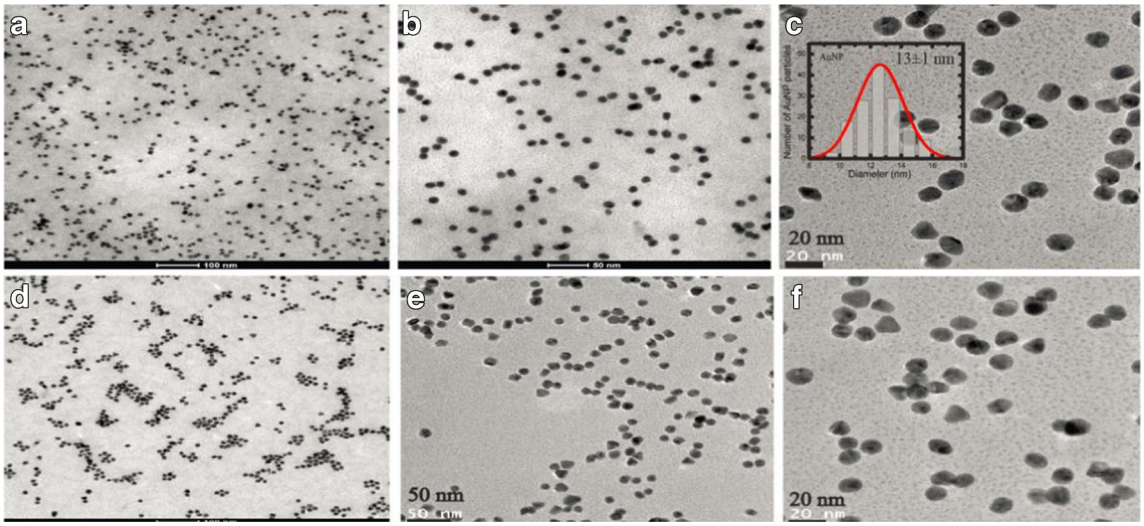

Fig. 2 The TEM images of GNPs dispersion (**a**–**c**) and peptide-coated GNPs dispersion without any aggregation (**d**–**f**), and the *inset* shows the diameter distribution of GNPs (**a**)

diameter distribution of the GNPs was measured using a TEM images analysis. The average diameter of the GNPs, which were found to be 13 ± 1.0 nm (Fig. 2), was measured by statistical analysis of normal distribution. The TEM images of peptide-coated GNPs (PC-GNPs) were shown in Fig. 2d–f. Peptide capping does not affect the gold nanoparticle size if gold nanoparticles do not aggregate during the assembly process. On the basis of the TEM images, and the constant gold core diameter, it is evident that PC-GNPs remain monodisperse after capping (Fig. 2d–f).

The HR-TEM image (Fig. 3a–c) of GNPs showed that the fringe spacing of GNP was 2.5 A°, which corresponded to the spacing between the plane of face-centered cubic (fcc) gold. The selected area of the diffraction pattern (SEAD) of gold nanoprism (Fig. 3d) indicated that the entire nanoparticle was monocrystalline structure [30]. The pattern of SEAD was indexed according to planes of (111) and (200) reflection of fcc gold on the basis of the d-spacing 2.4 and 2.04 A°. The d-spacing were also calculated from diffraction pattern which varied from 1.84 to 2.27 A°. The HR-TEM image of peptide-coated GNPs showed (Fig. 3b) that the thin layer of peptide coating was observed. The FTIR spectra of citrate-stabilized GNPs was performed to know about molecules present on the surface and showed the FTIR spectra

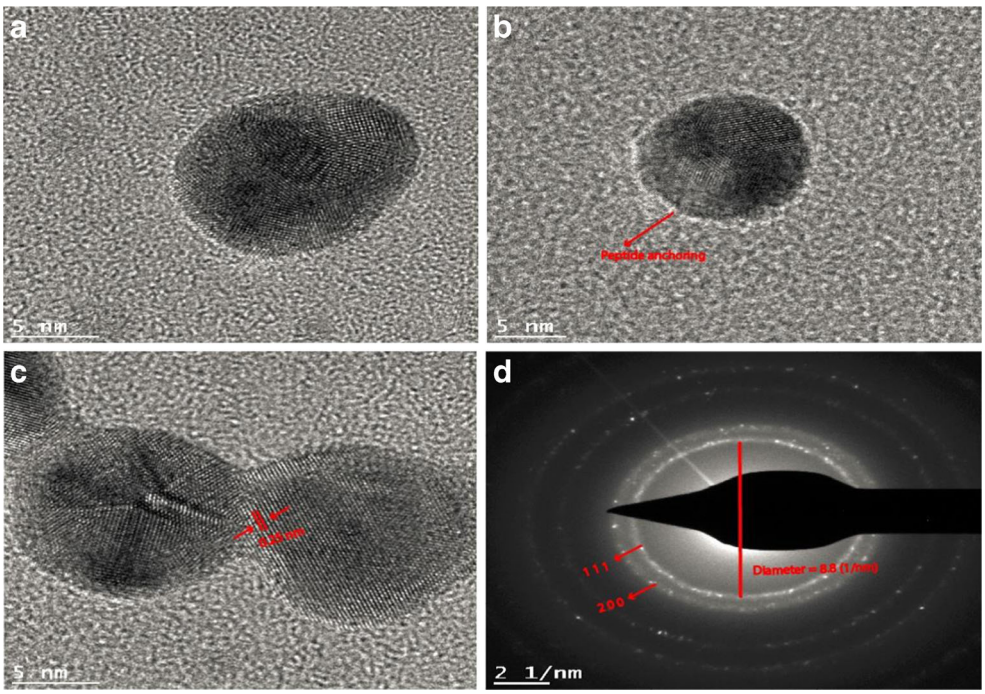

Fig. 3 **a** HR-TEM image of gold nanoparticle. **b** TEM image of peptide-coated GNP. **c** HR-TEM image of gold nanoprism and showing a fringe spacing of 2.5 A°. **d** A selected area of diffraction pattern of gold nanoparticles

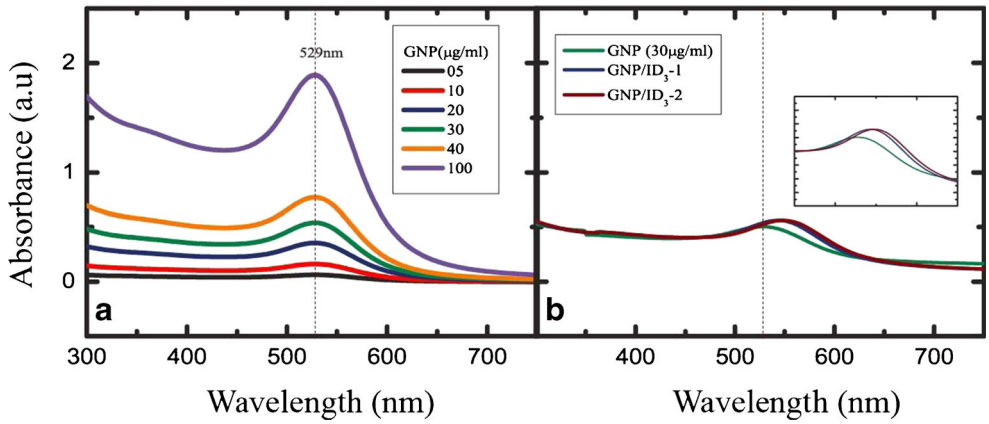

Fig. 4 **a** Absorption spectra peak intensity of GNPs at different concentrations. **b** Absorption spectra of GNPs and GNP/ID_3 at 30 mg/mL GNPs concentration

(Fig. S1a) obtained the GNPs showing several absorption peaks at 918, 1398, 1585, 1667, and 3352 cm^{-1}. The fluorescence spectra of GNP solution (5 μg/mL) performed with different excitation wavelengths from 370 to 420 nm are displayed in Fig. S2a. The peak position of the photoluminescence (PL) band appears from 423 to 439 nm wavelengths. An increase of peak intensity with decreasing excitation wavelength was observed. The intensity of the emission band was increased with increased GNP concentration, and the trend was consistent with the changes corresponding to the surface plasmon band of GNPs (Fig. S2b). The optical properties of gold are due to the 5d valence and 6sp conduction electrons. The outermost d and s electrons of the constituent atoms must be treated together leading to six bands. The single-photon luminescence from gold has been described [31, 32].

From UV-visible, citrated GNPs show a plasmon band at 529 nm (Fig. 4a). The particle diameter can also be calculated from the concentration of gold nanoparticles and the absorbance at the surface plasmon resonance and is in agreement with a diameter of 13 nm [33]. The surface plasmon absorption spectrum of GNP as the function of concentration is shown in Fig. 4a. The intensity of absorption spectra increased with increasing GNP concentration. The trend was consistent with the changes corresponding to the surface plasmon band of GNPs. For peptide (ID_3)-coated GNPs, the plasmon band absorbance shifts to higher wavelength 550 nm.

The hydrodynamic diameter of PC-GNPs was measured by Zetasizer to be 15.0 ± 0.5 nm. Zeta potential measurements indicate that the charge of the Cit-GNP is −37 ± 1.8 mV (Fig. 5) in water and the charge of PC-GNPs is −17 ± 0.5 mV. The differences observed between citrated GNPs and PC-GNPs in UV-visible, TEM, and zeta potential measurements show evidence that the peptide is effectively capping the GNPs. The shift to a higher plasmon band, and the hydrodynamic diameter size increase by about 1–2 nm after addition of peptide is consistent with the formation of a peptide layer on the surface of GNPs [18]. Also, the reduction of charge from −37 to −17 mV (Fig. 5) indicates the displacement of negatively charged citric acid by the peptide. The slightly negative charge remaining on the PC-GNPs is most

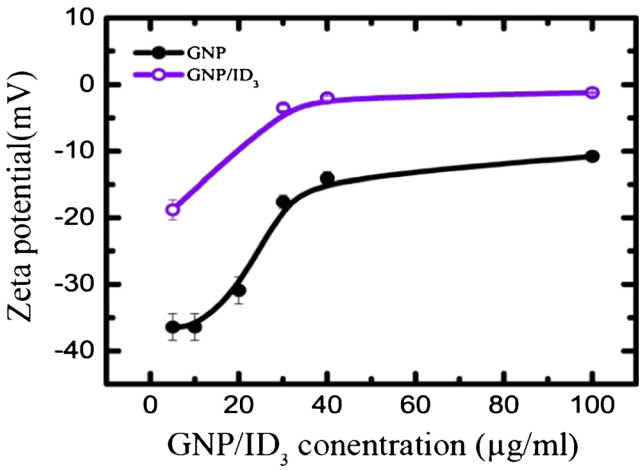

Fig. 5 The zeta potential of GNPs and GNP/ID_3 as the function of concentration

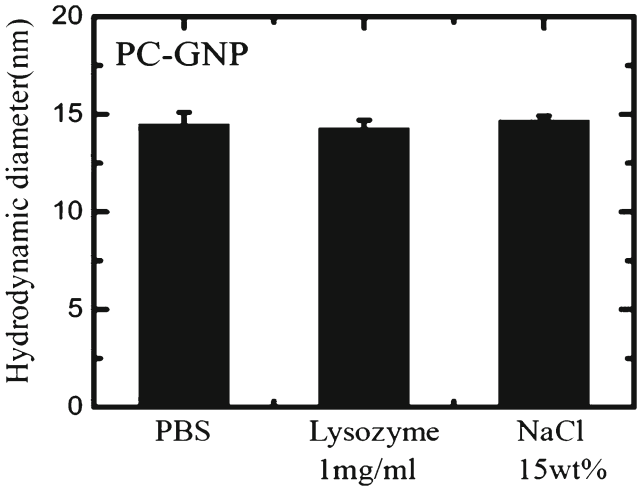

Fig. 6 DLS measurements of the hydrodynamic diameter (volume percentage) (nm) of PC-GNPs after exposure to PBS, 1 mg/mL lysozyme in PBS, and 15 wt% NaCl solution for 50 min. Each data point represents an average value/standard deviation from three independent measurements

likely due to a small amount of residual citrate molecules remaining on the surface after ligand exchange.

Stability in phosphate-buffered saline (PBS) is the first criteria for developing a robust, biocompatible system. However, if particles are to be utilized in more complex environments, such as in vivo, then harsher conditions need to be evaluated. Particle stability was assessed by monitoring the hydrodynamic diameter of particles using UV-visible, TEM, and DLS. As seen in Fig. 6, PC-GNPs maintain the same hydrodynamic diameter after exposure to 15 wt% NaCl, 1 mg/mL lysozyme, and PBS solutions.

We examined PC-GNP stability under high salt conditions. Most particles aggregate when the salt was added due to the screening of electrostatic repulsion; however, zwitterionic and mixed charge materials can resist aggregation due to the presence of a strongly bound surface hydration layer [17, 18]. In addition to examine particle stability in PBS solutions, the stability of PC-GNPs was also measured at higher salt concentrations. PC-GNPs maintain stability even at 15 (wt%) salt concentration. This result indicates the formation of a peptide-coated layer on the surface of gold nanoparticles.

Conclusion

In summary, the synthesis, characterization of gold nanoparticles capped with peptide material binding anchoring, was demonstrated. These materials were generated through a simple reduction approach, which provides a general synthetic route that produced particles of similar size using peptides of binding affinity. The GNPs were generally spherical with a relatively narrow size distribution. Peptide-coated GNPs shows high stability in high salt concentration without any aggregating. The results suggest that the reactivity of the peptide on GNPs surfaces is governed by the more details of the conformation of the bound peptide on the reconstructed nanoparticle surface as dictated by the peptide structure. These results may help for the use of peptides in the development of functional nanoparticles that exploit surface-based activity.

Acknowledgments The authors would like to thank WPI, USA, and IISc, Bangalore, India, for the financial support.

References

1. Baptista P, Pereira E, Eaton P, Doria G, Miranda A, Gomes I, Quaresma P, Franco R (2008) Anal Bioanal Chem 391(3):943–950
2. Dykman LA, Khlebtsov NG (2011) Acta Nat 3(2):34–55
3. Yeh YC, Creran B, Rotello VM (2012) Nanoscale 4(6):1871–1880
4. Han M, Gao X, Su JZ, Nie S (2001) Nat Biotechnol 19(7):631–635
5. Huang X, El-Sayed IH, Qian W, El-Sayed MA (2006) J Am Chem Soc 128(6):2115–2120
6. Mirkin CA, Letsinger RL, Mucic RC, Storhoff JJ (1996) Nature 382(6592):607–609
7. Moreno-Manas M, Pleixats R (2003) Acc Chem Res 36(8):638–643
8. Salem AK, Searson PC, Leong KW (2003) Nat Mater 2(10):668–671
9. Peng ZA, Peng X (2002) J Am Chem Soc 124(13):3343–3353
10. Puntes VF, Krishnan KM, Alivisatos AP (2001) Science 291(5511):2115–2117
11. Choi CHJ, Zuckerman JE, Webster P, Davis ME (2011) P Natl Acad Sci USA 108(16):6656–6661
12. Albanese A, Chan WC (2011) ACS Nano 5(7):5478–5489
13. Karmali PP, Simberg D (2011) Expert Opin Drug Del 8(3):343–357
14. Larson TA, Joshi PR, Sokolov K (2012) ACS Nano 6(10):9182–9190
15. Kodiyan A, Silva EA, Kim J, Aizenberg M, Mooney DJ (2012) ACS Nano 6(6):4796–4805
16. Liu XS, Chen YJ, Li H, Huang N, Jin Q, Ren KF, Ji J (2013) ACS Nano 7(7):6244–6257
17. Yang W, Zhang L, Wang SL, White AD, Jiang SY (2009) Biomaterials 30(29):5617–5621
18. Zhang L, Xue H, Gao CL, Carr L, Wang JN, Chu BC, Jiang SY (2010) Biomaterials 31(25):6582–6588
19. Collier JH, Segura T (2011) Biomaterials 32(18):4198–4204
20. Levy R, Thanh NTK, Doty RC, Hussain I, Nichols RJ, Schiffrin DJ, Brust M, Fernig DG (2004) J Am Chem Soc 126(32):10076–10084
21. Olmedo I, Araya E, Sanz F, Medina E, Arbiol J, Toledo P, Alvarez-Lueje A, Giralt E, Kogan MJ (2008) Bioconjug Chem 19(6):1154–1163
22. Morais T, Soares ME, Duarte JA, Soares L, Maia S, Gomes P, Pereira E, Fraga S, Carmo H, Bastos MDL (2012) Eur J Pharm Biopharm 80(1):185–193
23. Prades R, Guerrero S, Araya E, Molina C, Salas E, Zurita E, Selva J, Egea G, Lopez-Iglesias C, Teixido M, Kogan MJ, Giralt E (2012) Biomaterials 33(29):7194–7205
24. Arosio D, Manzoni L, Araldi EM, Scolastico C (2011) Bioconjug Chem 22(4):664–672
25. Kim YH, Jeon J, Hong SH, Rhim WK, Lee YS, Youn H, Chung JK, Lee MC, Lee DS, Kang KW, Nam JM (2011) Small 7(14):2052–2060
26. Scari G, Porta F, Fascio U, Avvakumova S, Dal Santo V, De Simone M, Saviano M, Leone M, Del Gatto A, Pedone C, Zaccaro L (2012) Bioconjug Chem 23(3):340–349
27. Sun L, Liu D, Wang Z (2008) Langmuir 24(18):10293–10297
28. Reithofer MR, Lakshmanan A, Ping AT, Chin JM, Hauser CA (2014) Biomaterials 35(26):7535–7542
29. Chen S, Cao Z, Jiang S (2009) Biomaterials 30(29):5892–5896
30. Mukherjee P, Senapati S, Mandal D, Ahmad A, Khan MI, Kumar R, Sastry M (2002) Chembiochem 3(5):461–463
31. Lin A, Son DH, Ahn IH, Song GH, Han WT (2007) Opt Express 15(10):6374–6379
32. Wang H, Huff TB, Zweifel DA, He W, Low PS, Wei A, Cheng JX (2005) Proc Natl Acad Sci U S A 102(44):15752–15756
33. Haiss W, Thanh NT, Aveyard J, Fernig DG (2007) Anal Chem 79(11):4215–4221